Pressure and Temperature Modulation in a Hot Isostatic Pressure Chamber

J. Tesoro, N. Jameel, A. Earley, P. Rassouli, Z. Ashraf

***Abstract*— Hot isostatic pressing (HIP) is a standard additive manufacturing process that is used to reduce the porosity of metal castings and ceramics, but in medical device manufacturing, is used often on biomedical implants. The ability to monitor and regulate temperature and pressure during a hot isostatic pressing cycle is critical to achieving the desired densification, ensuring implant biocompatibility and structural integrity. To optimize and automate the regulation of temperature and pressure during a HIP cycle, a PID-controlled system that injects an initial amount of gas, regulates the rate of temperature—pressure increase through thermal energy, then holds at a specified target is proposed. Utilizing the concepts of control theory, this work aims to theoretically characterize a HIP cycle as a dynamic biosystem by simulating PID control to determine if the temperature and pressure requirements of a desired HIP cycle are met. The results of our simulation suggest that this control system does have the potential to successfully monitor and regulate temperature and pressure levels during a HIP cycle, but it falls short as the system heats too rapidly. Possible future considerations are reducing simplifying assumptions and parameter optimization to approach a more realistic physical modeling of this system with a longer rise time. Regardless, this work still provides the theoretical background for modeling the temperature and pressure regulation of a HIP through subsequent controller design.**

***Clinical Relevance*—Hot Isostatic Pressing is imperative to ensure patient mobility, maintain biocompatibility, and improve the mechanical properties of bioimplants. Thus, it is essential the right pressure and temperature is applied to achieve patient needs.**

I. INTRODUCTION

The hot isostatic pressing (HIP) chamber is utilized for bioimplants post processing. The process of hot isostatically pressing the implants improves the implant's material microstructure by eliminating porosity. This is achieved by sustaining implants at very high pressure and temperature for an extended period, known as the soak time [1]. After this is achieved, the implant goes from about 99.5% dense from the 3D printer to around 99.99% dense [2]. The high pressure and temperature applied isostatically ensures the micro-air bubbles in the implants collapse without destroying or altering the original implant structure. Optimal hipping results are achieved at 1,172 K and 1,003 atm for 2 hours and 15 minutes per cycle [3]. First, the chamber must be fully vacuum sealed as atmospheric gases can react at such high temperatures and pressures, thereby causing material defects to the implants. To prevent surface reactions, argon gas is often used as the gas medium for its inert behavior and optimal thermal energy transfer. Temperature and pressure gain of the chamber is done through the input, thermal energy, which is achieved by induction coils to ensure thermal energy gain throughout the chamber. As for pressurizing, this is achieved by the argon gas once it is released into the chamber [4]. Ensuring uniform pressure from all directions is vital for preventing any deformation of the implant. The chamber is typically made from molybdenum which is strong enough to withstand high pressure and temperature. The chamber must gradually reach our target pressure and temperature because if this process is done too quickly, we will lose the isostatic properties leading to deformed implants. Once the cycle has run for its allocated time the system is cooled, and the pressure is slowly released. Similarly, it is crucial to slowly release the pressure and cool the system so as not deform the implant by breaking the isostatic properties inside the chamber.

This portion of the process is not covered in this report as the main focus is achieving our target pressure and temperature and keeping them steady for the whole cycle. This is where a proportional—integral—derivative (PID) controller is utilized with a pressure and temperature sensor so our system can correct and restabilize if it begins to sway from the required target parameters. Control was achieved through simplifying assumptions and subsequent ordinary differential equation (ODE) derivation for pressure and temperature to obtain a transfer function which calculates the PID coefficients, allowing for system characterization. The high pressure and temperature applied isostatically ensures the micro-air bubbles in the implants collapse without destroying or altering the original implant structure. In achieving predictable control, we ensure the implants are durable, resistant to corrosion, and biocompatible which all reduce the risk of adverse reactions within the body once implanted [5].

II. ODE FORMULATION

A. Assumptions

To obtain the ODE for pressure and temperature, we simplified the dynamics of the system's temperature-pressure regulation by making the following assumptions:

- Volume is cylindrical and incompressible.
- Thermal energy loss of the gas medium within the chamber and subsequent loss to the environment are considered separately.
- Thermal energy gain of the system is simplified to just the interior gas medium.

- Thermal energy loss is kept constant.
- Thermal energy gain and loss is uniform throughout the chamber surface area.
- Initial system temperature and pressure is based off after argon gas addition.
- External environment is at standard temperature and pressure (STP).

Thus, the control problem can be reduced to 2 processes:

1. Thermal energy input to increase system temperature-pressure until target conditions are met.
2. Balancing system thermal energy gain with thermal energy loss to the environment to sustain hipping at target for the soak time.

B. Pressure ODE Derivation

As argon gas is inert and exclusively the gas medium within the chamber, the ideal gas law (1) was used to model the relationship between temperature and pressure. Assuming that volume is incompressible:

$$PV = nRT \rightarrow P = \frac{nR}{V}T, \tag{1}$$

where n is the moles of Argon gas, R is the gas constant, V is volume, and T is temperature.

Since this pressure change is time-dependent, taking the derivative of pressure in (1) with respect to time yields the final ODE (2) for pressure:

$$\frac{dP}{dt} = \alpha \frac{dT}{dt}, \tag{2}$$

where $\alpha = \frac{nR}{V}$.

C. Temperature ODE Derivation

In considering thermal energy gain and loss within the chamber, both can be modeled by the equation describing thermal energy of a sample in (3) to characterize temperature dependency on heat:

$$q_{gain} = q_{loss} = mc_v\Delta T \rightarrow \Delta T = \frac{q}{mc_v} \tag{3}$$

where q is thermal energy, c_v is the specific heat capacity of Argon gas, m is the mass of argon gas, and ΔT is the temperature change from final to initial conditions.

Considering thermal energy is our driving force and time dependent, taking the derivative of (3) with respect to time yields the ODE (4) for temperature:

$$\frac{dT}{dt} = \frac{1}{mc_v}q(t) \tag{4}$$

However, (4) only describes thermal energy changes within the chamber itself. To quantify the thermal energy lost to the environment, the heat transfer through the molybdenum chamber material in (5) is formulated as follows:

$$Q = \frac{kA\Delta T}{L}, \tag{5}$$

where Q is the external heat transfer, k is the thermal conductivity of solid molybdenum, A is the surface area of a cylinder, ΔT is the temperature change from initial conditions relative to the current temperature at time t, and L is the chamber wall thickness. Note that A is not the cross-sectional area, but rather the surface area, due to the assumption of uniform thermal energy gain and loss across the chamber interface between the interior and exterior.

Therefore, the thermal energy loss consideration in (5) modifies (4) to completely characterize the temperature change driven by thermal energy, producing the final ODE (6) for temperature:

$$\frac{dT}{dt} = \beta(q(t) - Q\Delta t), \tag{6}$$

where $\beta = \frac{1}{mc_v}$ and Δt is the time step denoting the interval at which thermal energy is lost. Note that Δt is multiplied with Q to eliminate time dependency in adherence with the simplifying assumption of constant thermal energy loss, allowing for (6) to only have temperature K as it's SI unit.

III. Open Loop transfer function derivation and Bode Analysis

A. Derivation

The open loop transfer function is defined as the product of the transfer functions of the PID controller, the time delay of the measurement sensor, and the system. The PID controller transfer function is defined in (7) as

$$F(s) = \frac{K_d s^2 + K_p s + K_i}{s} \tag{7}$$

and the measurement sensor transfer function (8) is defined as

$$G(s) = \frac{1}{1 + \tau s}. \tag{8}$$

where τ is the time constant of the sensor. The first step in deriving the open loop transfer function is to define the input and output of our system to derive the system transfer function. We define the input of our system as thermal energy in the form of heat and our output as temperature. With the input and output defined, we perform a Laplace transform on (6) and derive (9), the transfer function $\frac{T(s)}{q(s)}$ to be:

$$H(s) = \frac{T(s)}{q(s)} = \frac{1}{s + \beta z\Delta t}, \tag{9}$$

where $z = \frac{kA}{L}$. Note that Q was deconstructed to isolate $T(s)$, notated as the new variable z. When the Laplace transform is performed, we can disregard the environmental temperature because it is not a value that is expected to change. Substituting our individual transfer functions into the open loop transfer function results in (10):

$$OL(s) = F(s)G(s)H(s) = \frac{K_d s^2 + K_p s + K_i}{s(1 + \tau s)(s + \beta z\Delta t)} \tag{10}$$

Additionally plugging in the known constants in Table 1 yields (11), the final form used to calculate the PID coefficients:

$$OL(s) = \frac{K_d s^2 + K_p s + K_i}{28409.1s^2 + 286590.4s + 24995} \quad (11)$$

Table I: Parameter Definitions

τ (seconds)	0.1
Δt (seconds)	0.5
β (K·J^{-1})	3.581808365527200e-06
z (J·s^{-1}K^{-1})	4.999051541836209e+04

For our system to be ideal, we want to cancel out the poles that are produced by the product of the transfer functions for our measurement sensor and our system. To do this we set K_d, K_p, and K_i equal to the constant values in the denominator of equation (11), so 28409.1, 286590.4, and 24995 respectively. Once those values are set and the two negative poles of the system are canceled out, the open loop transfer function simply reduces to (12):

$$OL(s) = \frac{1}{s} \quad (12)$$

B. Bode Analysis

The results of our open loop transfer function is a bode plot representative of a singular pole at zero. This is attributed to the open loop transfer function resulting in three poles, where two of which were negative and one at zero, and two zeros. However, to enhance the stability of our PID controlled system, we decided to cancel out the two negative poles with the two zeros. Looking at figure 3 which demonstrates the bode plot for the derived open loop transfer function, we see that our system is a singular pole, decreasing 20 dB/decade starting at zero. More importantly from the open loop transfer function and the resulting bode plot, we observe that our system is indeed stable. The transfer function doesn't result in any positive poles that would indicate instability and the phase plot of the bode in figure 1 tells us that there is a phase margin of 90º, which also indicated a very stable system. In addition to the stability of our system, from our open loop result, we also find there to be zero DC error since the gain is infinite at zero, as shown in the magnitude plot in figure 1.

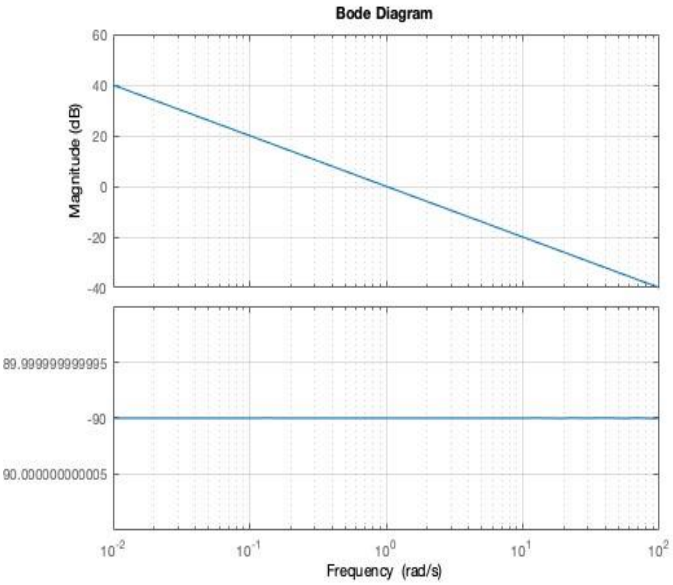

Figure 1: Open loop transfer function bode plot, demonstrating the magnitude and phase in relation to frequency.

IV. Closed Loop transfer function derivation and Analysis

A. Derivation and Analysis

After deriving the open loop transfer function OL(s) in (10), the standard closed loop transfer function can be obtained through (13):

$$CL(s) = \frac{OL(s)}{1 + OL(s)}. \quad (13)$$

If we plug in equation (10) into equation (13) and simplify, we found the finalized closed loop transfer function to be:

$$CL(s) = \frac{K_d s^2 + K_p s + K_i}{\frac{\tau s^3}{\beta} + \left(\frac{1}{\beta} + \tau z \Delta t + K_d\right) s^2 + \left(z\Delta t + K_p\right) s + K_i}, \quad (14)$$

whereby plugging in the values of all the known constants from Table 1 in (14), the finalized version of the closed loop transfer function is derived as:

$$CL(s) = \frac{27917.4s^2 + 281673.2s + 24995.25}{27917.4s^3 + 309590.5s^2 + 306668.4s + 24995.25} \quad (15)$$

For the closed loop transfer function in (15), we ended up finding that all poles were real and negative, indicating that the closed loop system, when taking into consideration the effect of feedback and time delay, was still stable. The poles for the closed loop system were found to be: -0.08953, -1, and -9.999984.

IV. Block Diagram and Simulink Results

A. *Block Diagram*

Figure 2 displays the Simulink block diagram that models the temperature control for our HIP Chamber. The step block represents the heat input to the system and represents the target temperature values that we desire the HIP to stabilize and hold at for an extended period. The gain values represent the constants α and β in our final theoretical model of temperature (6) and the final conversion of the output temperature to pressure using (1). Also seen in Figure 1 is the implementation of the time delay transfer function G(s) from (8) and the incorporation of the PID controller block which is used to correct for the error during the HIP cycle. There is also the addition of a constant block to account for the initial environmental temperature and pressure assumed to be at STP.

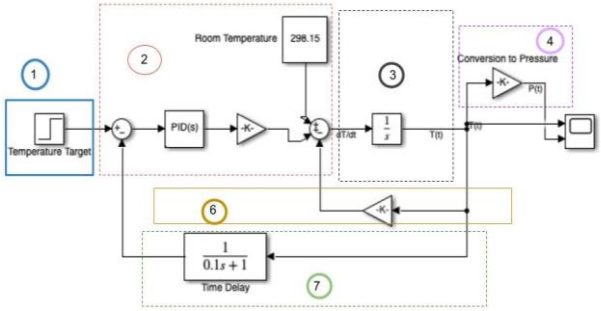

Figure 2: Simulink divided into Each Functional Section: (1) the input, (2) Calculation of dT/dt through heat gain and heat loss using a feedback loop and the gain value of beta, (3) The conversion of the signal into temperature, (4) the conversion of the signal into pressure using a gain of alpha, (6) the feedback loop of temperature, and (7) the time delay (0.1s).

B. *Simulation Results*

After running the simulation of our block diagram through Simulink, our resulting temperature and pressure profile is shown in Figure 4. The simulation was run for a time step of 100, which represents a 100-minute HIP cycle because of the units used for the Simulink model.

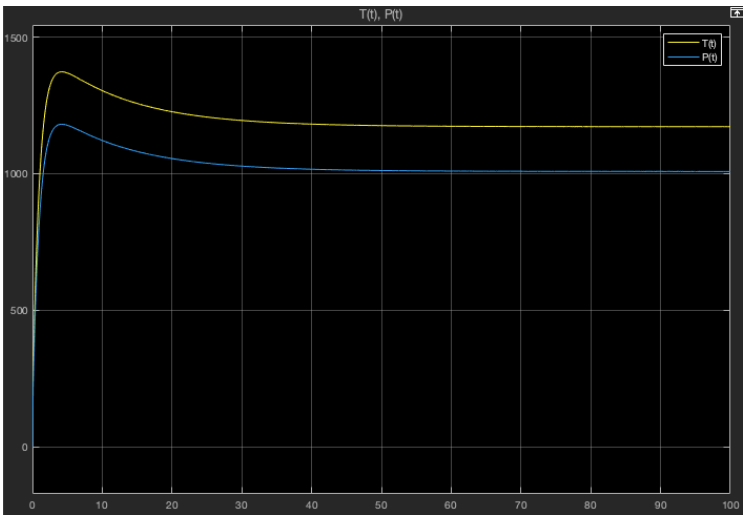

Figure 3: Pressure in blue (atm) and Temperature in yellow (K) vs. Time (min).

V. Discussion and Future Considerations

In figure 3, both the curves for pressure and temperature shoot up and then stabilize very quickly. At the beginning of the curve, heat gain is significantly greater than heat loss, causing a rise in pressure and temperature (which are proportionally related). The curves shoot up and eventually overshoot past the target for both pressure and temperature, mainly due to the time delay in our system. After overshooting, heat gain approaches heat loss and this allows the system to lower and stabilize to our target values for pressure and temperature. Every measurement made from the system is not reported at the exact time its occurring, due to measurement time delay. The behavior of the system is very similar to an ideal system but occurs very quickly (5 minutes). This could be very risky for our HIP Chamber to handle a very fast change in temperature and pressure in the real world and could possibly be a safety hazard as rapid heating could cause bioimplant defects. A rapid increase in temperature and pressure caused by non-uniform heating results in thermal stresses leading to uneven material contractions that compromises structural integrity. This behavior is the result of a very high integral coefficient in the PID controller. Parameter optimization could be a possible solution, this could decrease the amount of argon gas, increase volume, increase the pressure reach, and thus lead to a lower Ki value in the PID controller.

Acknowledgment

We would like to extend our gratitude to Professor Cauwenberghs for a great quarter in learning biosystem control theory. We are forever grateful for his passion and dedication for teaching. We would also like to thank our TA, Benjamin Balster, for helping these concepts for providing feedback and support during our time in the course. Finally, we would like to express our gratitude to our senior project mentor Jeff Brittan for guiding us through this design process.

REFERENCES

[1] "Hot Isostatic Pressing." *Hot Isostatic Pressing - an Overview | ScienceDirect Topics*, www.sciencedirect.com/topics/engineering/hot-isostatic-pressing. Accessed 13 Dec. 2023.

[2] Watershed Ideas Foundry Inc. "Materials Testing and Evaluation."

[3] Kittyhawk Inc. "Cycle Completed within Tolerance of Cycle Parameters and Customer Required Temperature Indicated." 11651 Monarch St Garden Grove , 17 Oct. 2023.

[4] Ageev, S. V., and V. L. Girshov. "Hot Isostatic Pressing of Metal Powders - Metallurgist." *SpringerLink*, Springer US, 8 Dec. 2015, link.springer.com/article/10.1007/s11015-015-0153-y.

[5] "Biomedical Device Densification." *Pressure Technology, Inc.*, www.pressuretechnology.com/hip-applications-biomedical.php#:~:text=The%20medical%20industry%20utilizes%20Hot,and%20the%20potential%20for%20corrosion. Accessed 13 Dec. 2023.